

Supplemental Tables and Figures

Table S1. In vitro kinase inhibition by allosteric Akt inhibitor, AKTi

| Isozyme | Recombinant enzyme assay IC ₅₀ (nM) | | Cell culture assay [*] EC ₅₀ (nM) | |
|-----------|---|-----------|--|-----------|
| | Human | Mouse | Human | Mouse |
| Akt1 | 3.5 ± 1.5 | 6.0 ± 3.4 | 12.5 ± 6.0 | 26 ± 12 |
| Akt2 | 40 ± 11 | 58 ± 5.3 | 460 ± 240 | 970 ± 520 |
| Akt3 | 1,900 ± 460 | nd † | 4,800 ± 2,300 | nd |
| Akt1ΔPH ‡ | >50,000 | nd | nd | nd |

^{*} Inhibition of Akt activation in human C33a cells and mouse MMT060562 cells treated with AKTi, as measured in kinase assays of individual immuno-captured Akt isozyms (average and standard deviation of at least three independent experiments)

† Not determined

‡ Recombinant Akt1 kinase lacking the PH domain

Table S2: Counterscreen results at 10 μ M AKTi

| Enzyme | % activity | Enzyme | % activity | Enzyme | % activity |
|------------------|------------|---------------------|------------|--------------------|------------|
| Abl(h) | 96 | Flt3(h) | 54 | PDK1(h) | 135 |
| Abl(T315I)(h) | 109 | Fms(h) | 101 | Pim-1(h) | 62 |
| ALK(h) | 66 | Fyn(h) | 86 | Pim-2(h) | 100 |
| ALK4(h) | 99 | GSK3 α (h) | 100 | PKA(h) | 109 |
| AMPK(r) | 103 | GSK3 β (h) | 92 | PKB α (h) | 0.004* |
| Arg(h) | 88 | Hck(h) | 63 | PKB β (h) | 0.04* |
| ASK1(h) | 95 | HIPK2(h) | 98 | PKB γ (h) | 1.9* |
| Aurora-A(h) | 87 | IGF-1R(h) | 95 | PKC α (h) | 94 |
| Axl(h) | 64 | IKK α (h) | 103 | PKC β I(h) | 104 |
| Blk(m) | 52 | IKK β (h) | 113 | PKC β II(h) | 99 |
| Bmx(h) | 83 | IR(h) | 103 | PKC γ (h) | 77 |
| BRK(h) | 66 | IRAK4(h) | 86 | PKC δ (h) | 46 |
| BTK(h) | 86 | JAK3(h) | 88 | PKC ϵ (h) | 73 |
| c-RAF(h) | 82 | JNK1 α 1(h) | 98 | PKC η (h) | 72 |
| CaMKII(r) | 101 | JNK2 α 2(h) | 98 | PKC ι (h) | 83 |
| CaMKIV(h) | 99 | JNK3(h) | 84 | PKC μ (h) | 68 |
| CDK1/cyclinB(h) | 81 | KDR(h) | 90 | PKC θ (h) | 57 |
| CDK2/cyclinA(h) | 104 | Lck(h) | 86 | PKC ζ (h) | 99 |
| CDK2/cyclinE(h) | 83 | Lyn(h) | 36 | PKD2(h) | 87 |
| CDK3/cyclinE(h) | 99 | MAPK1(h) | 106 | Plk3(h) | 115 |
| CDK5/p35(h) | 99 | MAPK2(h) | 104 | PRAK(h) | 104 |
| CDK6/cyclinD3(h) | 100 | MAPKAP-K2(h) | 103 | PRK2(h) | 86 |
| CDK7/cyclinH(h) | 98 | MAPKAP-K3(h) | 95 | Pyk2(h) | 78 |
| CHK1(h) | 99 | MEK1(h) | 101 | Ret(h) | 46 |
| CHK2(h) | 96 | MELK(h) | 100 | RIPK2(h) | 97 |
| CK1 δ (h) | 78 | Met(h) | 127 | ROCK-I(h) | 56 |
| CK1(y) | 78 | MINK(h) | 106 | ROCK-II(h) | 6.1* |
| CK2(h) | 98 | MKK4(m) | 104 | Ron(h) | 110 |
| cKit(D816V)(h) | 51 | MKK6(h) | 116 | Ros(h) | 91 |
| cKit(h) | 162 | MKK7 β (h) | 96 | Rse(h) | 85 |
| CSK(h) | 94 | MPKK1(rab) | 69 | Rsk1(h) | 79 |
| CSNK1(r) | 75 | MSK1(h) | 92 | Rsk2(h) | 68 |
| CSNK2(h) | 95 | MSK2(h) | 72 | Rsk3(h) | 59 |
| cSRC(h) | 82 | MST1(h) | 49 | SAPK2a(h) | 87 |
| DDR2(h) | 95 | MST2(h) | 71 | SAPK2b(h) | 103 |
| DYRK1A(r) | 68 | NEK2(h) | 75 | SAPK3(h) | 100 |
| EGFR(h) | 100 | NEK6(h) | 93 | SAPK4(h) | 103 |
| EphA2(h) | 92 | NEK7(h) | 101 | SGK(h) | 76 |
| EphA4(h) | 79 | p38a(h) | 95 | Syk(h) | 77 |
| EphB2(h) | 26 | p38b(h) | 97 | TAK1(h) | 82 |
| EphB4(h) | 51 | p38g(h) | 85 | TBK1(h) | 99 |
| ErbB4(h) | 64 | p38d(h) | 81 | Tie2(h) | 60 |
| Fer(h) | 85 | p70S6K(h) | 49 | TrkA(h) | 22 |
| Fes(h) | 62 | p70S6KB1(h) | 52 | TrkB(h) | 64 |
| FGFR1(h) | 92 | PAK2(h) | 94 | Yes(h) | 67 |
| FGFR2(h) | 99 | PAK4(h) | 5.2* | ZAP-70(h) | 144 |
| FGFR3(h) | 80 | PAR-1B α (h) | 77 | ZIPK(h) | 97 |
| FGFR4(h) | 35 | PDGFR α (h) | 45 | | |
| Fgr(h) | 70 | PDGFR β (h) | 58 | | |
| Flt1(h) | 14 | PDK1(h) | 135 | | |

* IC50 value [μ M]

Figure S1: Structure of naphthyridinone AKTi

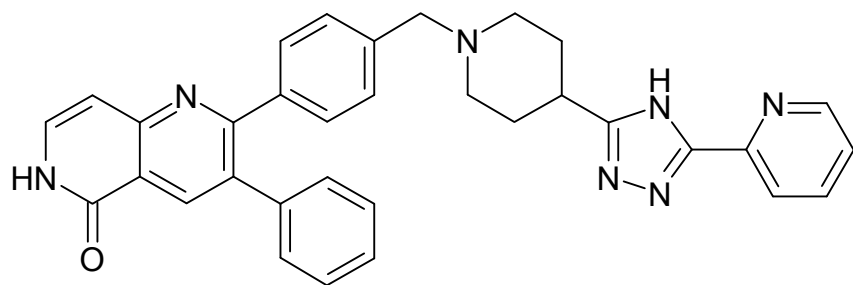
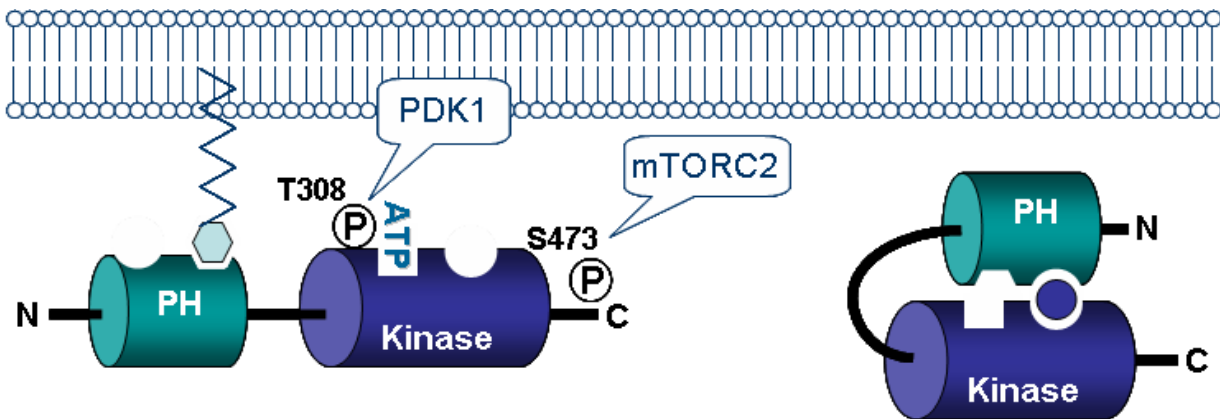
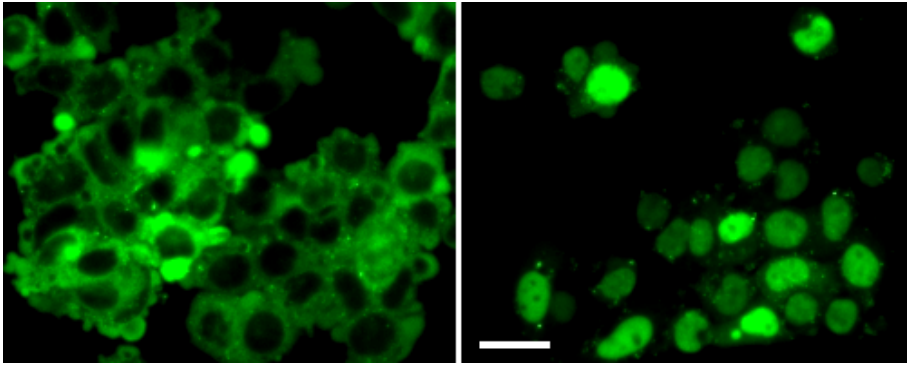


Figure S2 : Model of Akt activation



In the absence of inhibitors, the PH domain of Akt interacts with PIP3 in the plasma membrane and is phosphorylated by PDK1 on T308 in the activation loop and by mTORC2 on S473 in the regulatory C-terminal tail. AKTi binding (blue circle) to a hypothetical site formed by the juxtaposition of PH and kinase domains induces a closed, inactive conformation.

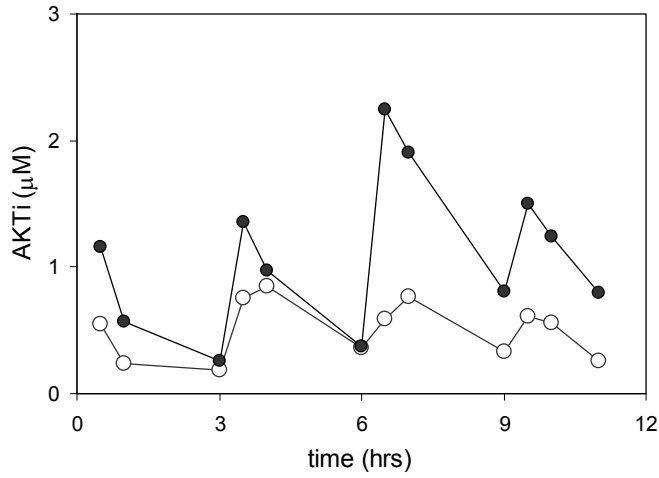
Figure S3 : Akt inhibition allows nuclear translocation of FKHRL-1



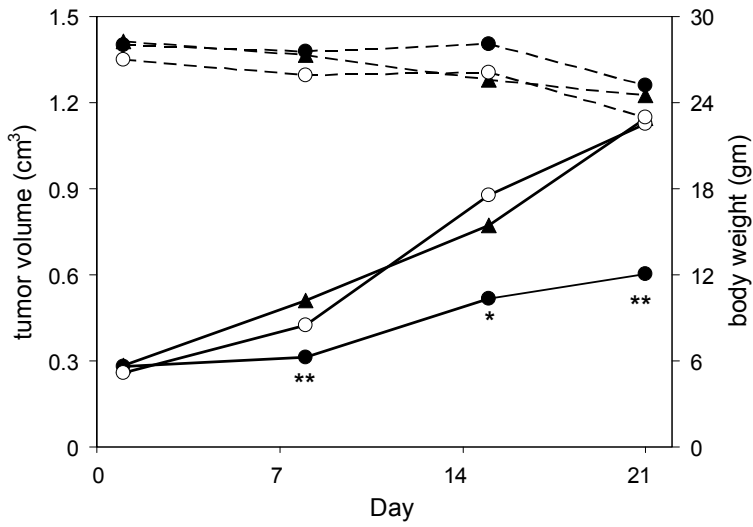
C33a (GFP-FKHRL-1) cells were treated with 15 μ M AKTi (right panel) or vehicle (left panel) for 1.5 hrs. Nuclei were stained with DAPI. Images were taken with an InCell Analyzer 1000 at 20x Q505LP dichroic magnification (bar = 25 nm). Quantitation by InCell imaging yielded an EC_{50} value for inhibition of cytoplasmic retention of 2.4 μ M. See Supplemental methods for details.

Figure S4: Efficacy study with LNCaP xenografts with weekly dosing of AKTi

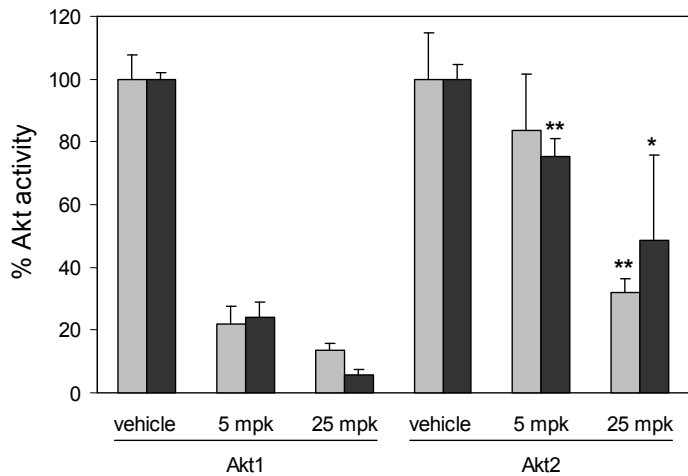
A



B

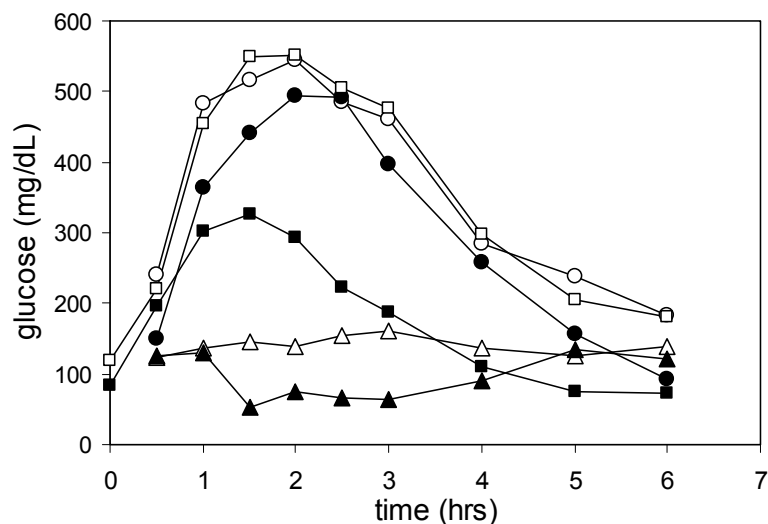


C



LNCaP tumor-bearing mice were dosed with 20 mpk or 100 mpk of AKTi, once weekly for three weeks. Compound was administered as four subcutaneous doses of 4x 5 mpk or 4x 25 mpk, respectively, at 3-hour intervals. (A) Blood concentrations of AKTi in 4x 5 mpk group (open circles) and 4x 25 mpk group (filled circles); averages of 3 animals per group. (B) Time course of tumor volumes (solid lines) and animal weights (dashed lines) of treated animals (symbols as above) and vehicles controls (triangles). Values represent averages from 10 animals per group. Asterisks denote p-values of < 0.05 (*) and < 0.005 (**) versus the vehicle group (one-tailed unpaired t-test). (C) Inhibition of Akt1 and Akt2 in lung (grey bars) and LNCaP tumors (black bars). Tissues were harvested two hours after the last injection on week 3. Akt isozyme activities were measured by IP-kinase assay in homogenized tissues and normalized against the vehicle control group. Values and error bars represent averages and standard deviations of three animals per group. Asterisks denote p-values as shown above.

Figure S5: Impact of fasting and exogenous insulin on blood glucose levels following AKTi treatment



Mice were fasted overnight (filled squares) and or left with food (open squares), followed by subcutaneous administration of a single 100-mpk dose of AKTi. In an independent experiment non-fasted mice were administered a single 100-mpk dose of AKTi (circles) or vehicle (triangles), followed one hour later by an intraperitoneal injection of 40 μ g insulin (filled symbols) or vehicle (open symbols). Blood glucose levels were measured at the indicated times starting 30 min after insulin injection.

Supplemental Methods

Forkhead translocation

C33a cells expressing a forkhead-GFP fusion protein (FKHRL-1-GFP) were generated as follows: FKHRL-1 cDNA from human kidney (GenBank Accession # U55763) was cloned into pEGFP-C1 (Clontech #6084-1) and transfected into C33a cells using Lipofectamine 2000 (Invitrogen), followed by selection of stable clones with 400 μ g/mL G418 (Invitrogen). C33a (FKHRL-1-GFP) cells were cultured in α -MEM with 10% FBS. For translocation assays, cells were seeded at 1×10^5 cells/well in 96-well format. After incubation for 24 hrs, 0.2 to 15 μ M AKTi in growth media was added for 1.5 hrs. Media was removed and cells were fixed with 4% paraformaldehyde for 20 min at room temperature. Fixed cells were washed with PBS and incubated with 3 μ M DAPI (Molecular Probes) for 1 hr. Cells were imaged using the InCell Analyzer 1000 (GE Biosciences) at 20x Q505LP dichroic magnification.

Analysis of AKTi concentrations in mouse blood

Mouse blood was collected via tail vein bleeding at specified times and immediately placed on dry ice. AKTi concentrations were determined by LC-MS/MS in positive ion mode using the Turbo Ion Spray interface at 450 degrees C. Blood samples (10 μ L) containing an internal standard (25 μ L of AKTi control) were protein-precipitated by adding 50 μ L of acetonitrile with 0.1% formic acid. After centrifugation, 50 μ L of supernatant was transferred to a 96-well plate and diluted by adding 100 μ L of water containing 0.1% formic acid. 12- μ L aliquots were injected into the Sciex API 4000 LC-MS/MS system. Chromatography was performed using a Supelco Discovery C18, 5cm x 2.1m, 5 micron column. Quantitation was based on selected reaction monitoring of precursor/product ion pair m/z 540 – 311.